Environmental Science
Water Research & Technology

Ferric tannate photothermal material for efficient water distillation

Journal:	*Environmental Science: Water Research & Technology*
Manuscript ID	EW-COM-11-2019-001016.R2
Article Type:	Communication

SCHOLARONE™
Manuscripts

Solar distillation based on an interfacial photothermal material provides a sustainable way to acquire fresh water from saline and polluted water. This work demonstrate the potential of a low-cost natural material, ferric tannate in solar steam generation and fabricated a photothermal composite membrane stabilized by atomic layer deposition.

COMMUNICATION

Ferric tannate photothermal material for efficient water distillation

Received 00th January 20xx,
Accepted 00th January 20xx

DOI: 10.1039/x0xx00000x

Cheng Zhang,[a] Zhaowei Chen,[b] Zijing Xia,[a,c] Ruben Z. Waldman,[a,c] Shao-Lin Wu,[d] Hao-Cheng Yang,[d]* and Seth B. Darling[a,c,e]*

Utilizing sunlight to accelerate water evaporation is emerging as a promising strategy for desalination and for distilling wastewater. Here we report on the application of ferric tannate as such a photothermal material, which is deposited onto a polyvinylidene fluoride (PVDF) membrane and encapsulated with titanium dioxide via atomic layer deposition. This system achieves 63.9% efficiency for the overall process, suggesting strong potential for real-world application.

Shortages of fit-for-purpose water are becoming increasingly prevalent in regions around the globe, driven by climate disruption, development, and rapid urbanization. Since traditional direct resources like rivers, lakes, and aquifers cannot satisfy the growing demand of freshwater, emerging technologies such as distillation and membrane-based separation have been developed to attain freshwater from increasingly challenging sources such as wastewater or seawater. Unfortunately, these technologies consume a vast amount of energy during the purification processes, posing a difficult choice between energy and water. A distinct, but related, challenge is residuals management from resource extraction operations (e.g. hydraulic fracturing), where large-scale evaporation ponds often represent a bottleneck in productivity due to the slow-paced reduction in wastewater volume. Recently, a novel technology, often referred to as solar steam generation, has emerged to realize polluted/saline water purification by utilizing solar energy, which may help alleviate both freshwater and energy stresses. During this process, photothermal materials play a crucial role in light-to-heat conversion.

Conventional photothermal materials include carbon materials (e.g. carbon nanotubes,[1-2] graphene,[3-9] covalent organic frameworks,[10] and carbonized organic materials[11]), plasmonic metals (e.g. Au[12,13] and Al[14] nanoparticles), semiconductors (e.g. MXene[15], MoS_2[16]) and natural black compounds[17]. However, most of these materials typically require complicated synthesis procedures, expensive precursors and equipment, or harsh fabrication conditions like high temperature, strong acidic/alkaline or oxygen-free environment. Natural materials are also of great interest in this field because they are easy-to-obtain and often environmentally friendly.[18] Therefore, significant effort has been devoted to developing novel photothermal materials with facile and green fabrication processes as well as non-toxic chemical components.

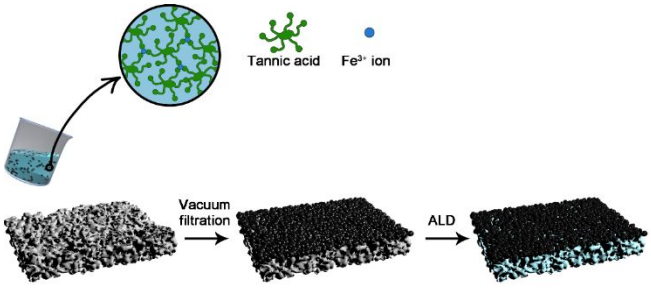

Scheme 1 Fabrication process of photothermal membrane coated with ferric tannate and encapsulated by ALD.

In our previous work, we demonstrated that traditional Chinese ink, as one of the earliest applied carbon nanomaterials, displays outstanding photothermal properties in solar steam generation.[19] Ferric tannate, an organic/inorganic composite complex and THE main ingredient of iron gall ink, therefore drew attention as a potential alternative option in photothermal application. Compared with

[a] Pritzker School of Molecular Engineering, University of Chicago, Chicago, IL, 60637, USA
[b] Center for Nanoscale Materials, Argonne National Laboratory, Lemont, IL 60439, USA.
[c] Advanced Materials for Energy-Water Systems (AMEWS) Energy Frontier Research Center, Argonne National Laboratory, Lemont, IL 60439, USA.
[d] School of Chemical Engineering and Technology & Southern Marine Science and Engineering Guangdong Laboratory (Zhuhai), Sun Yat-Sen University, Zhuhai, 519082, China.
[e] Center for Molecular Engineering & Chemical Sciences and Engineering Division, Argonne National Laboratory, Lemont, IL 60439, USA
Electronic Supplementary Information (ESI) available: [details of any supplementary information available should be included here]. See DOI: 10.1039/x0xx00000x

Chinese ink, it is more widely available, and its fabrication process is more convenient, simply involving the mixture of tannic acids (TAs) and iron salts. TA is a natural polyphenol extracted from plants, which can chelate with metal ions to form cross-linked complexes in aqueous solution. Herein, we fabricated a novel solar-steam-generating membrane by filtrating ferric tannate nano- and micro-particles onto a porous polyvinylidene fluoride (PVDF) membrane followed by atomic layer deposition (ALD) to stabilize the materials (**Scheme 1**). TiO_2 was selected for the ALD layer because it could be deposited under a relative low temperature (100 °C) to preserve the membrane structure, and its hydrophilic surface could facilitate the water transport onto the membrane surface. Moreover, titanium precursors can form coordination bonds with tannic acid, integrating the two materials and enhancing the stability of TiO_2 on the photothermal coating. The hydrophilic PVDF membranes are commercial products with an average pore size of 0.22 μm.

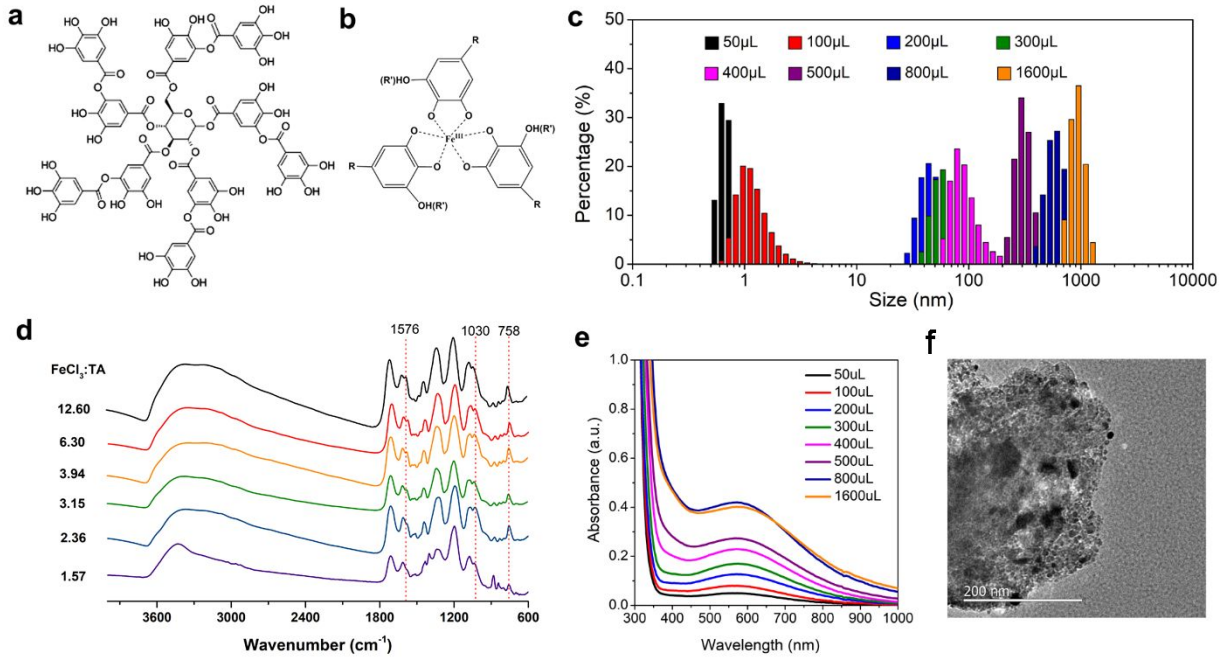

Figure 1. a) Molecular structure of tannic acid and b) ferric tannate complex. c) DLS size distribution of ferric tannate complex particles with different concentrations of iron chloride added. d) FTIR spectra of TA-Fe^{3+} complex with different $FeCl_3$/TA ratios. e) UV-vis-NIR spectrum of ferric tannate complex solutions. f) TEM image of a ferric tannate particle.

The solar steam generator is composed of a photothermal layer and a porous support layer, which is fabricated by filtrating ferric tannate (**Figure 1a,b**) nano- and micro-particles onto a porous membrane substrate. Nano- and micro-particles were synthesized by blending tannic acid with $FeCl_3$ in solution under mild stirring. TA can chelate with Fe^{3+} ions to form a 3D cross-linked network.[20] We first investigated the effect of $FeCl_3$/tannic acid ratio on the structure of the formed complex. The concentration of TA was fixed as 0.235 mM in a 20 mL solution. Different volumes of $FeCl_3$ solutions at a constant concentration of 37 mM were gradually dropped into TA solution under stirring, and the mixtures turned dark blue or black immediately once the two solutions encountered. The size of ferric tannate complexes was measured by dynamic light scattering (DLS). As shown in Figure 1c, the particle size increased from nanometer scale to micrometer scale with the addition of $FeCl_3$ solution. The rise of the particle size was caused by the growing cross-linking network under the condition of excess tannic acid. Specifically, the particle sizes ranged from 50 to 100 nm when the $FeCl_3$/TA ratio was between 1.57 and 3.15, whereas it dramatically increased to 300 nm at a $FeCl_3$/TA ratio of 3.93. The sharp growth of particle size was probably caused by coalescence. When the $FeCl_3$/TA ratio exceeded 12.6, significant large precipitates could be observed in the solution and the particle size reached ~1 μm. FTIR spectra of the TA-Fe^{3+} complex with different $FeCl_3$/TA ratio were revealed in **Figure 1d**. The black solid was collected by centrifugation and filtration of the suspension, and the complexes with low $FeCl_3$/TA ratio (0.39 and 0.78) were failed to be collected because they were too small. The spectra show no obvious changes when the $FeCl_3$/TA ratio exceeds 2.36, and the enhanced peaks at 1576 cm^{-1}, 1030 cm^{-1}, and 758 cm^{-1} indicate the formation of ferric tannate as revealed in previous reference.[21] FTIR spectra indicated that most of the particles were composed of ferric tannate when the $FeCl_3$/TA ratio exceed 2.36.

Since solar irradiation covers UV, visible, and near IR regions, we measured the UV-vis-NIR spectra of the ferric tannate solutions to evaluate their light absorption properties. The ferric tannate dispersions showed wide absorption ranging from the UV to visible light regions with a peak at around 570 nm (**Figure 1e**), similar to the spectrum for the analogous Fe-catechol complexes.[22,23] No significant shift of the peak was observed for complexes with different particle sizes, and absorbance increased with the addition of $FeCl_3$ solution because more complexes were formed in the solution. TEM imaging (**Figure 1f**) revealed that the ferric tannate

This journal is © The Royal Society of Chemistry 20xx

Please do not adjust margins

microparticles were composed of agglomerates of small nanoparticles.

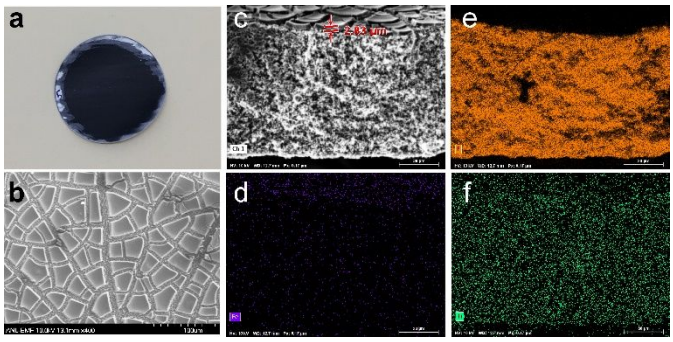

Figure 2. a) Digital picture of ferric-tannate-coated PVDF membrane. b) SEM top-view image and c-f) EDS mapping of the cross-section of ferric-tannate-coated PVDF membrane with TiO_2 ALD coating.

Due to the large inefficiency of a bulk heating configuration, interfacial heating is considered a superior strategy to enhance the efficiency by isolating heat at the evaporation interface. To this end, the prepared particles were filtrated on a hydrophilic PVDF membrane (**Figure 2a**), followed by 30 ALD cycles of TiO_2 to impart stability to the otherwise water-soluble coating. As shown in **Figure 2b**, micrometer-wide cracks appeared on the obtained ferric tannate coating after drying, which was caused by shrinkage of the rigid coating during the process. These cracks provide a rough surface, which can improve the absorption of sunlight via scattering and simultaneously provide channels to vertically transport water during the evaporation process. Energy dispersive spectroscopy (EDS) mapping (**Figure 2d-f**) indicates the TiO_2 ALD layer was deposited throughout the entire membrane. Such uniform TiO_2 coating formed on the ferric tannate coated-membrane acted as a "glue" to integrate the coating with the substrate against re-dispersion in water.

In our following test to evaluate stability, the membrane was immersed in water and put on an oscillator for two minutes. No material was observed to release from the membrane (**Figure 3a**). Beyond its encapsulation function, TiO_2 also hydrophilizes the material interface due to its plentiful hydroxide groups on the surface.[17] Water contact angle measurements indicated that the surface became highly hydrophilic, and water drops permeated through the membrane quickly (**Figure 3b**). During evaporation, such a hydrophilic surface would facilitate water transport due to the enhanced capillary effect.

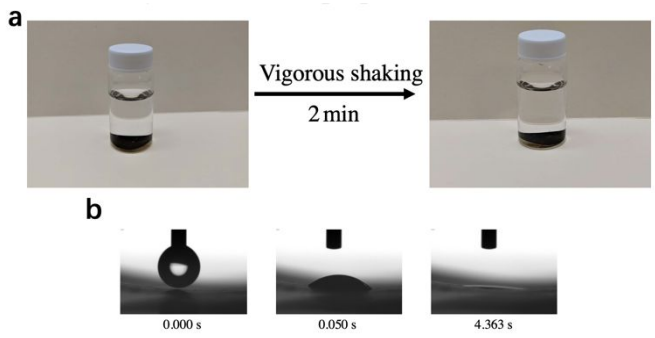

Figure 3. a) Two minutes of vigorous agitation on an orbital shaker does not detach the coating from the membrane. b) A water drop rapidly permeates through the ALD/ferric tannate membrane.

Solid UV-vis-NIR spectra can reveal the light absorption capacity of the obtained materials. According to the UV-Vis-NIR spectrum of a membrane in the dry state shown in **Figure 4a**, the absorption region overlaps well with the bulk of standard solar irradiation. Significantly, the absorption from 382 nm to 749 nm is over 90%, which is the highest-intensity irradiation region of sunlight. Thermogravimetric analysis (TGA) showed that more than 95% of the weight was maintained below 157 °C (the small weight loss was caused by the escape of water, **Figure S1**), indicating the excellent stability of ferric tannate complexes under high temperature. Regarding stability and cyclability, the temperature curve of the dry state membrane under repeated irradiation **(Figure 4b**) exhibits consistent, reproducible thermal generation ability.

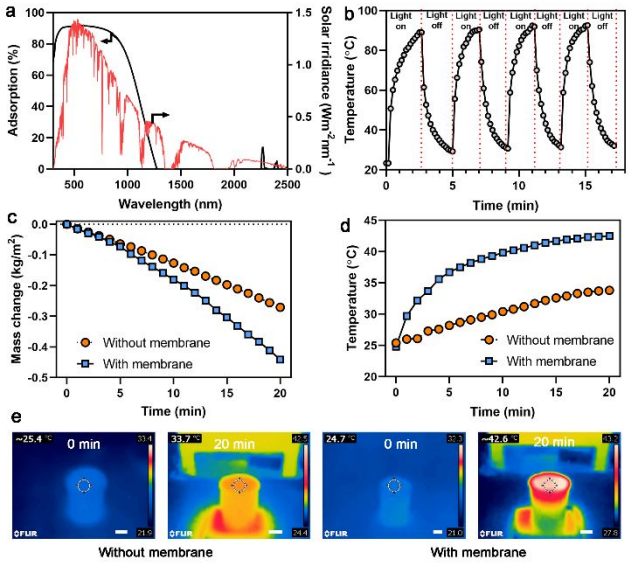

Figure 4. a) Solid UV-vis-NIR spectrum of ALD/ferric tannate membrane. b) Temperature evolution of ALD/ferric tannate membrane with/without the light. c) Mass and d) temperature changes of water with and without ALD/ferric tannate membrane. e) Infrared images of beakers with and without ALD/ferric tannate membrane before and after illumination. The scale bar is 10 mm.

In order to assess the photothermal performance of this device, relevant parameters were measured under the illumination of a simulated solar source. The irradiance power was controlled to be approximately one sun. As shown in **Figure 4c**, a benchmark measurement revealed 0.271 kg/m^2 of pure water was evaporated after 20 min irradiation, while the mass change reached 0.441 kg/m^2 when covering the coated membrane onto the surface. The thermal efficiency is calculated as ~63.9% according to the formula:

$$\eta_{th} = \frac{\Delta m h_{LV}}{C_{opt} I}$$

where η_{th} is solar thermal conversion efficiency, Δm is the mass loss of water at steady state (corrected for mass loss in the dark), h_{LV} is the total enthalpy of the liquid-vapor phase change (sensible heat + phase-change enthalpy), C_{opt} is the optical concentration (1.6 in this work) and I is the power density of solar illumination (1 kW/m^2). For comparison, the calculated evaporation efficiency of bulk water is

~33.2%. The evaporation efficiency was improved by using this photothermal material, however, even higher process efficiencies have been reported for carbon-based materials, such as Chinese ink that we reported previously.[19] Compared with Chinese ink, the ferric tannate shows nearly no absorption in the near infrared region as revealed in the solid UV-vis-NIR spectra (**Figure 4a**), leading to a reduction of light-harvesting efficiency. It should be mentioned the evaporation rate of a surface covered by a nascent PVDF membrane is similar to that of an uncovered water surface (**Figure S2**). In principle, the white PVDF membrane will enhance light reflection and reduce evaporation. However, because the membrane we used is hydrophilic, it will be fully wetted by the water, and there is a layer of water on the membrane surface, leading to a similar performance to the nascent water surface.

As one would anticipate based on these mass loss data, the membrane also showed a higher temperature change compared with water itself (**Figure 4d**). We also observed that, due to the thermal insulation effect of the substrate, there was an approximately 8.9 °C distinction between the surface and the bulk phase (**Figure 4e**). The dramatic temperature change validates the application potential of the ferric tannate complexes as photothermal materials. (The highest and lowest temperature of each scan progressively increased, which can be explained by some thermal conduction to the bulk water.)

Conclusions

We have demonstrated the fabrication of a highly effective solar steam generation device based on ferric tannate and ALD interface engineering.[24] The high efficiency and reusability of the device under simulated sunlight, resulting from its combination of effective light harvesting, efficient photothermal conversion, good fluid transport, and stability in water, highlights the promise of this material for water distillation applications.

Conflicts of interest

There are no conflicts to declare.

Acknowledgement

This work was supported as part of the Advanced Materials for Energy-Water Systems (AMEWS) Center, an Energy Frontier Research Center funded by the U.S. Department of Energy, Office of Science, Basic Energy Sciences. Use of the Center for Nanoscale Materials, an Office of Science user facility, was supported by the U.S. Department of Energy, Office of Science, Office of Basic Energy Sciences, under Contract No. DE-AC02-06CH11357. H.-C. Yang also acknowledges financial support from the National Natural Science Foundation of China (51909291) and Fundamental Research Funds for the Central Universities (19lgzd17).

Notes and references

1 Y. Wang, L. Zhang, P. Wang, Self-Floating Carbon Nanotube Membrane on Macroporous Silica Substrate for Highly Efficient Solar-Driven Interfacial Water Evaporation, *ACS Sustain. Chem. Eng.* **2016,** *4*, 1223-1230.

2 Y. Yang, X. Yang, L. Fu, M. Zou, A. Cao, Y. Du, Q. Yuan, C. -H.Yan, Two-Dimensional Flexible Bilayer Janus Membrane for Advanced Photothermal Water Desalination, *ACS Energy Let.* **2018,** *3*, 1165-1171.

3 X. Wang, G. Ou, N. Wang, H. Wu, Graphene-based Recyclable Photo-Absorbers for High-Efficiency Seawater Desalination, *ACS Appl. Mater. Interfaces* **2016,** *8*, 9194-9199.

4 J. Lou, Y. Liu, Z. Wang, D. Zhao, C. Song, J. Wu, N. Dasgupta, W. Zhang, D. Zhang, P. Tao, W. Shang, T. Deng, Bioinspired Multifunctional Paper-Based rGO Composites for Solar-Driven Clean Water Generation, *ACS Appl. Mater. Interfaces* **2016,** *8*, 14628-14636.

5 K. –K. Liu, Q. Jiang, S. Tadepalli, R. Raliya, P. Biswas, R. R. Naik, S. Singamaneni, Wood-Graphene Oxide Composite for Highly Efficient Solar Steam Generation and Desalination, *ACS Appl. Mater. Interfaces* **2017,** *9*, 7675-7681.

6 Y. Yang, R. Zhao, T. Zhang, K. Zhao, P. Xiao, Y. Ma, P. M. Ajayan, G. Shi, Y. Chen, Graphene-Based Standalone Solar Energy Converter for Water Desalination and Purification, *ACS Nano* **2018,** *12*, 829-835.

7 H. Ren, M. Tang, B. Guan, K. Wang, J. Yang, F. Wang, M. Wang, J. Shan, Z. Chen, D. Wei, H. Peng, Z. Liu, Hierarchical Graphene Foam for Efficient Omnidirectional Solar-Thermal Energy Conversion, *Adv. Mater.* **2017,** *29*, 1702590.

8 X. Hu, W. Xu, L. Zhou, Y. Tan, Y. Wang, S. Zhu, J. Zhu, Tailoring Graphene Oxide-Based Aerogels for Efficient Solar Steam Generation under One Sun, *Adv. Mater.* **2017,** *29*, 1604031.

9 X. Li, W. Xu, M. Tang, L. Zhou, B. Zhu, S. Zhu, J. Zhu, Graphene oxide-based efficient and scalable solar desalination under one sun with a confined 2D water path, *Proc. Natl. Acad. Sci. USA* **2016,** *113*, 13953-13958.

10 Z. –J. Xia, H. –C. Yang, Z. Chen, R. Z. Waldman, Y. Zhao, C. Zhang, S. N. Paterl, S. B. Darling, Porphyrin Covalent Organic Framework (POF)-Based Interface Engineering for Solar Steam Generation, *Adv. Mater. Interfaces* **2019**, *6*, 1900254.

11 T. Li, H. Liu, X. Zhao, G. Chen, J. Dai, G. Pastel, C. Jia, C. Chen, E. Hitz, D. Siddhartha, R. Yang, L. Hu, Scalable and Highly Efficient Mesoporous Wood ‐ Based Solar Steam Generation Device: Localized Heat, Rapid Water Transport, *Adv. Funct. Mater.* **2018,** *28*, 1707134.

12 L. Zhou, Y. Tan, D. Ji, B. Zhu, P. Zhang, J. Xu, Q. Gan, Z. Yu, J. Zhu, Self-assembly of highly efficient, broadband plasmonic absorbers for solar steam generation, *Sci. Adv.* **2016,** *2*, e1501227.

13 C. Chang, C. Yang, Y. Liu, P. Tao, C. Song, W. Shang, J. Wu, T. Deng, Efficient Solar-Thermal Energy Harvest Driven by Interfacial Plasmonic Heating-Assisted Evaporation, *ACS Appl. Mater. Interfaces* **2016,** *8*, 23412-23418.

14 L. Zhou, Y. Tan, J. Wang, W. Xu, Y. Yuan, W. Cai, S. Zhu, J. Zhu, 3D self-assembly of aluminium nanoparticles for plasmon-enhanced solar desalination, *Nat. Photonics* **2016,** *10*, 393.

15 R. Li, L. Zhang, L. Shi, P. Wang, MXene Ti_3C_2: An Effective 2D Light-to-Heat Conversion Material, *ACS Nano* **2017,** *11*, 3752-3759.

16 X. Yang, Y. Yang, L. Fu, M. Zou, Z. Li, A. Cao, Q. Yuan, An Ultrathin Flexible 2D Membrane Based on Single-Walled Nanotube ‐ MoS_2 Hybrid Film for High-Performance Solar Steam Generation, *Adv. Funct. Mater.* **2018,** *28*, 1704505.

17 M. Alberghini, M. Morciano, L. Bergamasco, M. Fasano, L. Lavagna, G. Humbert, E. Sani, M. Pavese, E. Chiavazzo, P. Asinari, Coffee-based colloids for direct solar absorption, *Sci. Rep.* **2019**, 9, 4701.

This journal is © The Royal Society of Chemistry 20xx

Please do not adjust margins

18 N. Xu, X. Hu, W. Xu, X. Li, L. Zhou, S. Zhu, J. Zhu, Mushrooms as Efficient Solar Steam Generation Devices, *Adv. Mater.* **2017,** *29*, 1606762.
19 H.-C. Yang, Z. Chen, Y. Xie, J. Wang, J. W. Elam, W. Li, S. B. Darling, Chinese Ink: A Powerful Photothermal Material for Solar Steam Generation, *Adv. Mater. Interfaces* **2019,** *6*, 1801252.
20 H. Ejima, J. J. Richardson, K. Liang, J. P. Best, M. P. van Koeverden, G. K. Such, J. Cui, F. Caruso, One-Step Assembly of Coordination Complexes for Versatile Film and Particle Engineering, *Science* **2013,** *341*, 154-157.
21 J. Iglesias, E. G. de Saldaña, J. A. Jaén, On the Tannic Acid Interaction with Metallic Iron, *Hyperfine Interact*. **2001**, 134, 109–114.
22 T. Liu, M. Zhang, W. Liu, X. Zeng, X. Song, X. Yang, X. Zhang, J. Feng, Metal Ion/Tannic Acid Assembly as a Versatile Photothermal Platform in Engineering Multimodal Nanotheranostics for Advanced Applications, *ACS Nano* **2018,** *12*, 3917-3927.
23 H. Xu, J. Nishida, W. Ma, H. Wu, M. Kobayashi, H. Otsuka, A. Takahara, Competition between Oxidation and Coordination in Cross-Linking of Polystyrene Copolymer Containing Catechol Groups, *ACS Macro Let.* **2012,** *1*, 457-460.
24 S. B. Darling, Perspective: Interfacial materials at the interface of energy and water, *J. Appl. Phys.* **2018,** *124*, 030901.

Table of Content

Ferric tannate is used as a photothermal material and integrated with a polymer membrane by atomic layer deposition for solar water distillation.